

MTA Facility Proposal for Beam Studies with the MICE Cavity

M. Backfish

March 7, 2016

1 Introduction

This document outlines the systems which will be used to deliver 400 MeV H-beam into the MTA facility for MICE cavity testing. Experiment mode configuration b, as described in the **MuCool Facility Shielding Assessment**, will be used for these tests [3]. In this mode of operation the shielding assessment states, “The proton beam is fully interacted by the experimental apparatus and the final beam absorber is not used.” The beam trajectory will be the same as configuration A which describes the trajectory when beam is cleanly transported to the final high-intensity beam absorber. This satisfies the trajectory requirement established on page 5 of of the shielding assessment. MICE cavity details are shown in figure 1 while the general configurations for the experimental apparatus are shown in figure 2 and 3.

The shielding assessment states on page 4 line 35, “Each experimental configuration will be individually evaluated based on its MOU and ORC, for compliance with the approved shielding assessment criteria.” The details in this document will be used to assist in evaluating the proposed experimental arrangement. First and foremost, the position of the new absorber will be evaluated geometrically with respect to experimental hall penetrations. Secondly, the additional beam travel will be evaluated to understand both the beam lattice and the impact of scattering over the added distance.

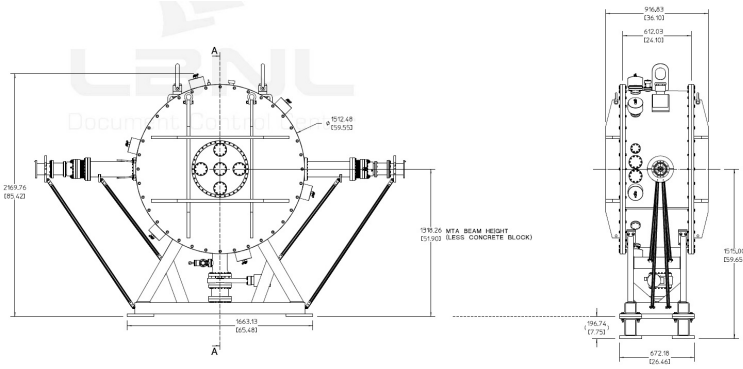


Figure 1: MICE Cavity

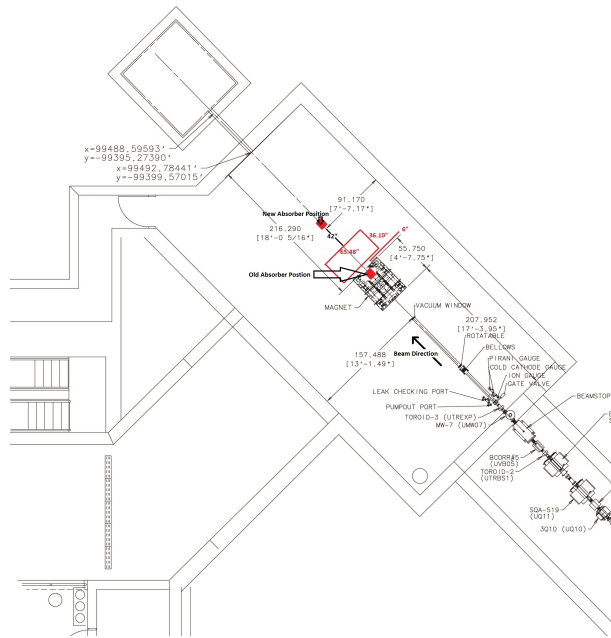


Figure 2: This overhead view of the configuration shows the approximate location of the MICE cavity. The beam absorber will be 1 m after the cavity as shown more specifically in figure 3

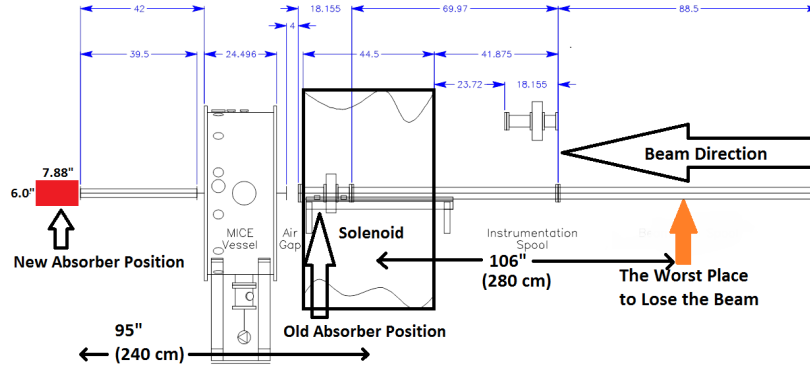


Figure 3: This side view of the new configuration shows beam pipe spool pieces. The beam absorber (shown in figure 4) will rest against the final downstream vacuum window flange.

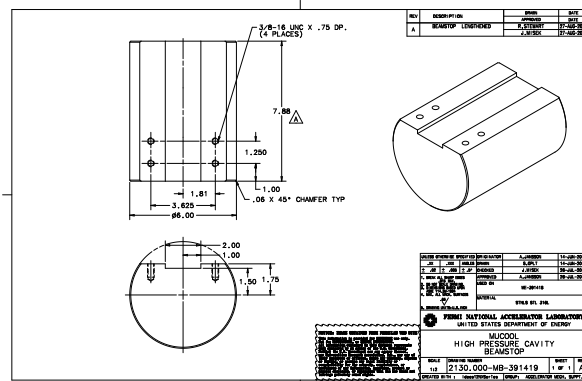


Figure 4: The Experimental Absorber being used is the same one used for prior High Pressure Cavity beam tests.

2 Radiation concerns regarding new beam geometries and how they impact experimental hall penetrations

TM-2248 states, “The scenario which describes the worst accidental beam loss occurs when the errant proton beam hits the beamline at $Z=-280$ cm (110 in) with a deflection angle of 50 mrad upward.” This scenario describes the overall worst case accidental beam loss. Figure 3 is labelled with the location of this worst case beam loss scenario. The new beam absorber configuration, described in figures 2 and 3, is 5 meters (201 in) further downstream from this worst case scenario position. The next sections will explain the the implications of this regarding penetrations.

2.1 Hatch Shield Wall, Ceiling Vent, and Gas Shed Penetrations

For the hatch shield wall the worst case scenario beam loss is 7 ft downstream of the absorber wall between linac and MTA [2]. The new experimental apparatus increases the distance between the beam absorber and this penetration by 95 in in comparison to the old absorber position as shown in figure 3. The added distance will reduce radiation levels. There is a vent on the North East corner of the ceiling in the largest section of the enclosure. A beam loss nearest to the ceiling vent provides the worst case scenario. The new experimental apparatus and absorber increases the distance between the ceiling vent and the final resting place for the beam by 95 in. The new experimental apparatus configuration and absorber also increases the distance from the gas shed penetrations by 95 in versus the old absorber position.

2.2 Refrigerator Room Cryo Penetrations

The Cryo penetrations must be evaluated cautiously as MARS simulations suggest the rates in the caged area in the refrigerator room in a worst case scenario could reach $9.06 * 10^{-2} \frac{mRem}{hour}$. These penetrations are of particular concern as the beam momentum occurs in the same general direction as the path that the penetrations take into the refrigerator room. The penetrations are shown in figure 5. The worst case scenario beam loss point is upstream of the solenoid. A small angle scatter could send beam closer to the penetrations. By increasing the distance from this worst case scenario, the angle between the beam and the penetration is increased. The vertical angle between the beam path at the old absorber and the cryo penetrations was 21° . The new absorber position increases this angle to 48° . The larger angle reduces the chances of a particle traveling into the penetration. The radiation levels in the penetration will be lower as a result. This penetration is monitored by a chipmunk and should be closely observed at low intensities as beam is established with the new configuration.



Figure 5: The cryo penetrations are in the top left corner of the downstream wall as circled in red in this image. By depositing the beam further downstream, the angle between the beam absorber and the penetrations is increased which decreases the chances of a particle passing directly into the penetration.

3 Lattice and Scattering Considerations

The beamline optics were designed with the ability to tune the focal point of the beam that is transmitted through the experimental hall. The model shown in figure 6 focuses the beam in both planes on the beamstop. This model shows that based on optical characteristics, beam can be delivered to the new experimental region without blowing up in transverse dimensions.

To limit scattering the beam will be under vacuum until it reaches the MICE cavity and as soon as it exits the MICE cavity as shown in figure 3. To determine the impact of this scattering on the beam as it travels to the beam stop we will determine the scattering angle for: the vacuum window before the MICE vessel, the MICE cavity upstream window, along with 2 beryllium windows that are inside the MICE vessel. The final section of beam pipe will be part of the MICE vacuum vessel. We will ignore the impact of the final vacuum window as there is effectively no distance between it and the final beam stop. The radiation length of a vacuum window made of TI-6AL-4V was calculated in Accelerator Beams Document 4697 [4]. The radiation length was found to be 3.7032 cm. The momentum of the Linac beam with Kinetic Energy 400 Mev is $954.691 \frac{MeV}{c}$. Relativistic β is thus .715. Using equation 1 from the PDG, a .007 cm window will cause a .0006 Radian scatter. The beam will pass through a second Ti window at the entrance to the MICE cavity which is .025 cm thick and will scatter .0015 Radians. The beam will then pass through 2 Beryllium windows each .038 cm thick. Thus each will scatter .00057 Radians.

To simplify the case we will look at the total scattering and consider it to occur at the first window which is 1.38 m from the beam stop. Note: this is a conservative estimate ignoring the fact that the other windows are further downstream. The total scattering angle is found by adding in quadrature all of the scattering contributions to get .0017 Radians. This angle propagated over 1.38 m results in .023 cm or 2.3 mm blowup.

Past MTA beam studies found the 1σ beam size to be 6 mm in the vertical plane and close to 3 mm horizontally [5]. Multiplying this by 3 to completely

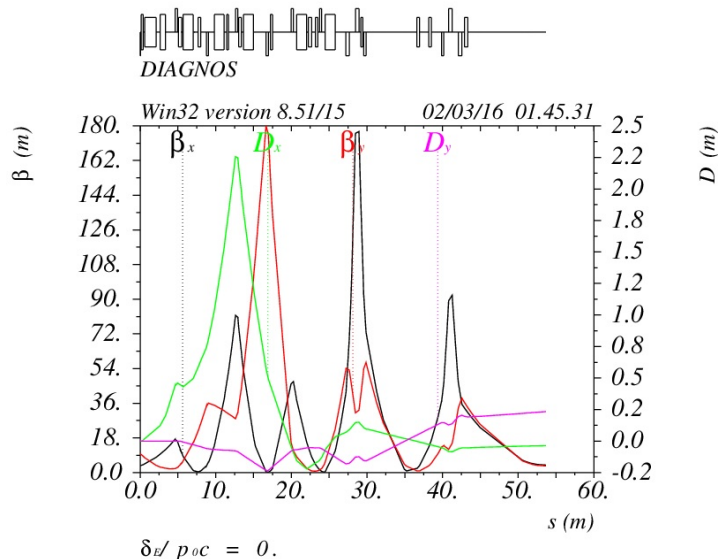


Figure 6: This MAD8 model shows the beamline parameters throughout the entire MTA beamline starting at the Linac versus their longitudinal position in the beamline labelled here as $s(m)$ and displayed in meters. In the absence of dispersion, the beam extent from the centroid is defined as $\sqrt{\beta * \epsilon}$ where ϵ is the beam emittance. The dispersion (D) is proportionally related to transverse beam size. The low β values and the low D values in this simulation suggest that the quadrupoles in the beamline can be tuned to properly deliver beam to the new absorber position. The solenoid is from 50.576 – 51.707 m. Vacuum window 1 is at 51.771 m. The MICE cavity is 51.872 – 52.196 m. Vacuum window 2 is at 52.53 m and vacuum window 3 is at 53.58 m just before the new absorber which is where the model ends above.

account for the beam half size gives a size of 9 mm or roughly 1 cm. The additional scattering results in 1.023 cm beam rather than 1 cm. The beam stop is 15 cm. These results suggest, the additional content in the beam path will not cause any significant scattering over the distance of beam travel thus scattering is not a concern for the MICE experimental apparatus.

3.1 Pressurizing the MICE cavity with nitrogen

The final step of the MICE cavity beam testing involves pressurizing the MICE cavity and the final section of beam pipe which will be connected to the MICE vessel with up to 2 atm of Nitrogen. This additional gas will cause an additional .00163 Radian scattering. Adding this in quadrature to the scattering from above gives a total scattering angle of .0024 Radians with the vertex shifted further downstream. Ignoring the downstream shift in vertex and calculating

as if the vertex is at the most upstream window (once again a very conservative estimate) we find the total scattering contribution at the beam stop is .033 cm or 3.3 mm. For this case the additional scattering results in 1.033 cm beam versus 1 cm, well within the limits of the 15 cm beamstop.

$$\theta_x = \frac{13.6}{PC * \beta} \sqrt{\frac{L}{L_r}} \left(1 + .038 * \log \sqrt{\frac{L}{L_r}} \right) \quad (1)$$

4 Conclusion

MICE cavity beam tests will provide valuable data which will be utilized as muon ionization cooling channels are created for MICE at Rutherford Appleton Laboratory. Analysis of the Fermilab MICE cavity in the MTA facility will complete the already successful MICE cavity testing program. The diligence of those who designed and built this facility resulted in an experimental hall capable of such tests. This document will be used in preparation for these tests. This document shows that radiation levels are reduced at the MTA penetrations as a result of the new experimental configuration. Profile monitors before and after the MICE cavity will be used to ensure the beam is properly delivered to the beam absorber.

References

- [1] C. Johnstone, I. Rakhno, N. Mokhov, W. Higgins, edited by M. Gerardi, “MuCOOL Facility Shielding Assessment”, Fermilab Batavia, Il Nov 1, 2010
- [2] I. Rakhno, C. Johnstone, “Radiation Shielding Calculations for MuCOOL Test Area at Fermilab”, Fermilab TM-2248, Batavia, Il May 2004
- [3] C. Johnstone, I. Rakhno, N. Mokhov, W. Higgins, edited by M. Gerardi, “MuCOOL Facility Shielding Assessment”, Fermilab Batavia, Il Nov 1, 2010
- [4] M. Backfish, “The Addition of an Air Gap in the Meson Test Secondary Beamline”, Beam Document 4697 Fermilab Batavia, Il Nov 5, 2014
Measurement of Transmission Efficiency for 400 MeV Proton Beam through Collimator at Fermilab MuCool Test Area Using Chromox-6 Scintillation Screen
- [5] M. R. Jana, M. Chung, B. Freemire, P. Hanlet, M. Leonova, A. Moretti, M. Palmer, T. Schwarz, A. Tollestrup, Y. Torun and K. Yonehara, “Measurement of Transmission Efficiency for 400 MeV Proton Beam through Collimator at Fermilab MuCool Test Area Using Chromox-6 Scintillation Screen”, Fermilab Batavia, Il Nov fermilab-pub-13-068, 2013